*Korean J. Chem. Eng.*, **31**(11), 1964-1972 (2014)
DOI: 10.1007/s11814-014-0121-4

pISSN: 0256-1115
eISSN: 1975-7220

# Experimental analysis and development of correlations for gas holdup in high pressure slurry co-current bubble columns

**Shyam Kumar and Ashok Khanna**†

Department of Chemical Engineering, IIT Kanpur, UP-208016, India
(*Received 20 September 2013 • accepted 21 April 2014*)

**Abstract**−The effect of liquid and gas velocities, solid concentrations, and operating pressure has been studied experimentally in a 15 cm diameter air-water-glass beads bubble column. The superficial gas and liquid velocities varied from 1.0 to 40.00 cm/s and 0 to 16.04 cm/s, respectively, while the solid loading varied from 1 to 9%. The gas holdup in the column was reduced sharply as we switched from batch to co-current mode of operation. At low gas velocity, the effect of liquid velocity was insignificant; while at high gas velocity, increasing liquid velocity decreased the gas holdup. Drift flux approach was applied to quantify the combined effect of liquid and gas velocities over gas holdup. For co-current three phase flows, the gas holdup decreased with increase in solid loading for all pressures. But for batch operations, when solid loading was 5% or more, settling started leading to higher gas holdup. Increasing pressure from atmospheric conditions increased the gas holdup significantly, flattening asymptotically.

Keywords: Multi Phase Flows, High Pressure, Gas Holdup, Drift Flux, Solid Concentration

## INTRODUCTION

A bubble column is a multiphase reactor in which the gas flows in the form of bubbles through the cylindrical reactor while liquid remains either stagnant (batch case) or also flows in the column. If the direction of the gas and liquid is the same, it is co-current flow. When solid particles are also present in the system, it is three phase flow. These types of reactors are used in chemical, petrochemical, biochemical and metallurgical industries [1]. Some of the examples include chemical processes involving reactions such as oxidation, chlorination, alkylation, polymerization and hydrogenation, biochemical processes like fermentation and biological wastewater treatment [2,3]. The advantages of this reactor over other multiphase reactors include less maintenance and low operating costs due to lack of moving parts, higher values of interfacial area and mass transfer coefficients, ability to handle solids, and high liquid residence time [2]. However, back mixing and complex hydrodynamics are the disadvantages. Average gas holdup is a dimensionless key parameter that characterizes the hydrodynamics inside the bubble column needed for design and scale up [4]. It is defined as the volume fraction of the column occupied by the gas bubbles. Variables affecting the gas holdup in a bubble column are liquid and gas velocities, solid concentration, operating pressure and column diameter [2,3]. The gas holdup does not depend upon column diameter for up-flow systems, if the diameter is greater than 15 cm [5].

The average gas holdup in a column has been estimated by many invasive and non-invasive techniques [6,7]. These include ultrasound, PIV, $\gamma$-ray, X-ray, laser Doppler anemometry, pressure drop measurements. Measuring the pressure drop using differential pressure transducer (DPT) is a low cost non-invasive technique, hence does not interrupt bubble column operation. Also, this technique does not necessarily need a transparent fluid, or electrolytic liquid [8]. It is used to measure the axial variation of the holdup in a column as well as the overall average gas holdup. Previous researchers have used it to calculate the gas holdup in two- and three-phase bubble columns [9,10].

Tang and Heindel [11] studied the effect of liquid velocity in a 15.24 cm diameter column [11]. They observed a decrease in holdup for co-current flows compared to batch experiments in a two-phase column. The effect of solid loading has been studied by various authors for a batch bubble column [12-17]. One group found a decreasing effect of solid loading over gas holdup [12,14-17]. The other group says that increasing solid loading first increases the gas holdup, and then after a certain value it decreases the holdup [13,18,19]. The presence of solid increases the mixture viscosity, which in turn increases the bubble size [20,21]. Further, the reduction of bubble breakup allows larger bubbles to increase in the column [22,23]. These large bubbles rise faster than small bubbles [12,17]. This decrease in the residence time leads to lower gas holdup. In the presence of solid, the increment in bubble population from small to large bubbles was also observed by Swart et al. [15]. Krishna et al. attributed the observed decrease in gas holdup to enhanced bubble coalescence with increasing slurry concentrations [24].

Gandhi et al. studied the effect of fine glass beads loading (35 μm) in water up to 40 vol% in discrete step of 10% on the gas holdup in a batch column [22]. They found that the average gas holdup initially decreases fast with increasing slurry concentration and the rate subsequently decreases for higher slurry concentrations. Kumar et al. performed experiments for three-phase flows at atmospheric conditions up to 16 cm/s gas velocity and found that the gas holdup remains nearly constant from batch case to up to 3% solid loading [25]. Afterwards it decreases when solid loading is increased. Mena et al. discussed the effect of solid loading (2.1 mm size with neutrally buoyant particle) varying from 1 to 30% in a batch column

†To whom correspondence should be addressed.
E-mail: akhanna@iitk.ac.in

[19]. They reported a dual effect of solid loading that increases the gas holdup for solid loading up to 3% and a decrease in holdup thereafter.

The gas hold-up increases as the pressure is increased [26,27]. Using the Kelvin-Helmholtz stability analysis, Letzel et al. showed that with increasing pressure, the surface of large bubbles become unstable for a wider range of wavelengths [27]. So, a dynamic equilibrium between bubble coalescence and bubble breakup shifts towards left at high pressures. Thus, the number of small bubbles increases in the column. Fan et al. showed that with an increase in pressure the rise velocity of bubbles decreases, which increases the gas holdup [16]. Li et al. showed that increase in pressure also decreases the bubble size formed by the sparger [28]. These three reasons allow the gas holdup to increase with increase in pressure. Gas holdup in a pressurized 0.162 m bubble column was studied by Kemoun et al. using $\gamma$-ray based computer tomography [29]. They also found that average gas holdup increases with pressure. Behkish et al. conducted experiments in a 29 cm diameter batch column for $N_2$ and He with Isopar-M, and reported that the gas holdup increases with increasing pressure, superficial gas velocity and temperature and decreases with increasing solid concentration [30]. All of these researchers studied high pressure experiments in batch operation mode only.

The drift flux approach originated by Zuber and Findlay and Wallis is a model which focuses on the relative velocity of the two phases [31,32]. Drift flux is defined as volumetric flux of either component relative to the surface moving at the average velocity [32]. The drift flux depends mainly on the gas velocity and slightly on the liquid velocity, the quality of the gas distributor, the particle sizes and the coalescence inhibiting behavior of the liquid [33]. The Zuber and Findlay drift-flux model has been used extensively in the literature to identify flow regime transitions and to predict the gas holdup in bubble columns by various researchers [2,6,31,33-35]. It accounts for the effects of radial non-uniformity of the local mixture flux density and the effect of the local relative velocity between the two phases [31].

Commercial slurry bubble columns are generally operated at high pressure and high solid (catalyst) loading to achieve high yields [24, 30,36]. These two conditions increase the productivity of the reactor [37] because high pressure insures higher gas solubility, and higher solid loading increases the reactant conversion. High pressure, high gas throughput, large reactor diameter and high slurry loadings are needed to achieve high space-time yields [38]. However, the effect of pressure for three-phase co-current systems has not been studied yet. Most of these literature studies are at atmospheric conditions. Few authors have studied high pressure bubble columns, and that too only for batch operations [30]. Thus, data for high pressure co-current bubble columns is inadequate in the literature. The objective of this research is to fill this gap experimentally. Experiments have been performed to investigate the effect of pressure, liquid and gas velocities, solid loading over gas holdup at high pressures. These experiments were performed for both low and high gas to liquid velocity ratio, while literature data mostly focuses on high gas to liquid velocity ratio. The relative importance of these parameters has also been evaluated. Drift flux approach has been used to correlate the gas holdup as a function of superficial gas and liquid velocities and to estimate the bubble diameter and its terminal rise velocity in both homogeneous and heterogeneous regimes. The effect of solid loading and liquid velocity over drift flux has also been evaluated. These effects have not been reported previously in the literature. Regression analysis has been performed to develop gas holdup correlations for both two- and three-phase flows at high pressures. These correlations have been converted into the non-dimensional form using dimensionless analysis of the bubble column.

## EXPERIMENTAL DETAILS

The experimental setup has been described in detail by Kumar et al. [39], so we will only briefly mention it here. A column of 15.4 cm diameter was fabricated using stainless steel (SS-304) that can sustain pressure up to 15 bar. The total height of the column is 2.72 m. Both gas and liquid phase enters the column from the bottom and flows in co-current mode. Differential pressure transducers (DPTs) have been placed at five locations to measure the pressure drop. Liquid flows through 3.75 cm pipe line, while air flows through 1.25 cm stainless steel (SS) pipe line. Compressed air was used as the gas phase and water as liquid phase. Glass beads of density 2,500 $kg/m^3$ were used as solid particles. The superficial gas velocity varied from 1.0 to 40.0 cm/s and superficial liquid velocity varied from 0 to 16.04 cm/s. Details of all the operating parameters are given in Table 1. A 1000 liter capacity tank made of SS-304 was used to store the water for recirculation. An agitator with two impellors was installed in the tank to properly mix the slurry. A mechanical seal was installed in the impeller shaft to stop the air leakage at high pressures during three phase experiments. Its dynamic part rotates with the impeller while the static part is fixed over the tank cover. Safety valves and pressure regulators were installed in the column and pipe line for safety purpose and to regulate the pressure in the column and tank. The schematic diagram of experimental setup is shown in Fig. 1.

Merchuk and Stein derived following equation to determine gas holdup in co-current flows [41]:

$$\varepsilon=1+\frac{dP}{\rho_l g dz}+\frac{4\tau_w}{\rho_l D_c g}+\frac{U_l^2}{g}\frac{1}{(1-\varepsilon)^2}\frac{d\varepsilon}{dz} \quad (1)$$

The second term in RHS is pressure drop due to gravity, the third

**Table 1. Parameters varied during experiments**

| | | | | | | | |
|---|---|---|---|---|---|---|---|
| Liquid velocity (cm/s) | 0 | 4.08 | 8.49 | 12.26 | 16.04 | | |
| Solid loading (wt%) | 0 | 1 | 3 | 5 | 7 | 9 | |
| Pressure (bar) | 1 | 3 | 5 | 7 | | | |
| Gas velocity (cm/s) | 1.13 | 2.26 | 3.4 | 4.53 | 5.66 | 6.79 | 7.93 |
| | 9.06 | 10.19 | 11.32 | 14.15 | 16.99 | 19.82 | 22.65 |
| | 25.48 | 28.31 | 31.14 | 33.97 | 36.80 | 39.63 | |

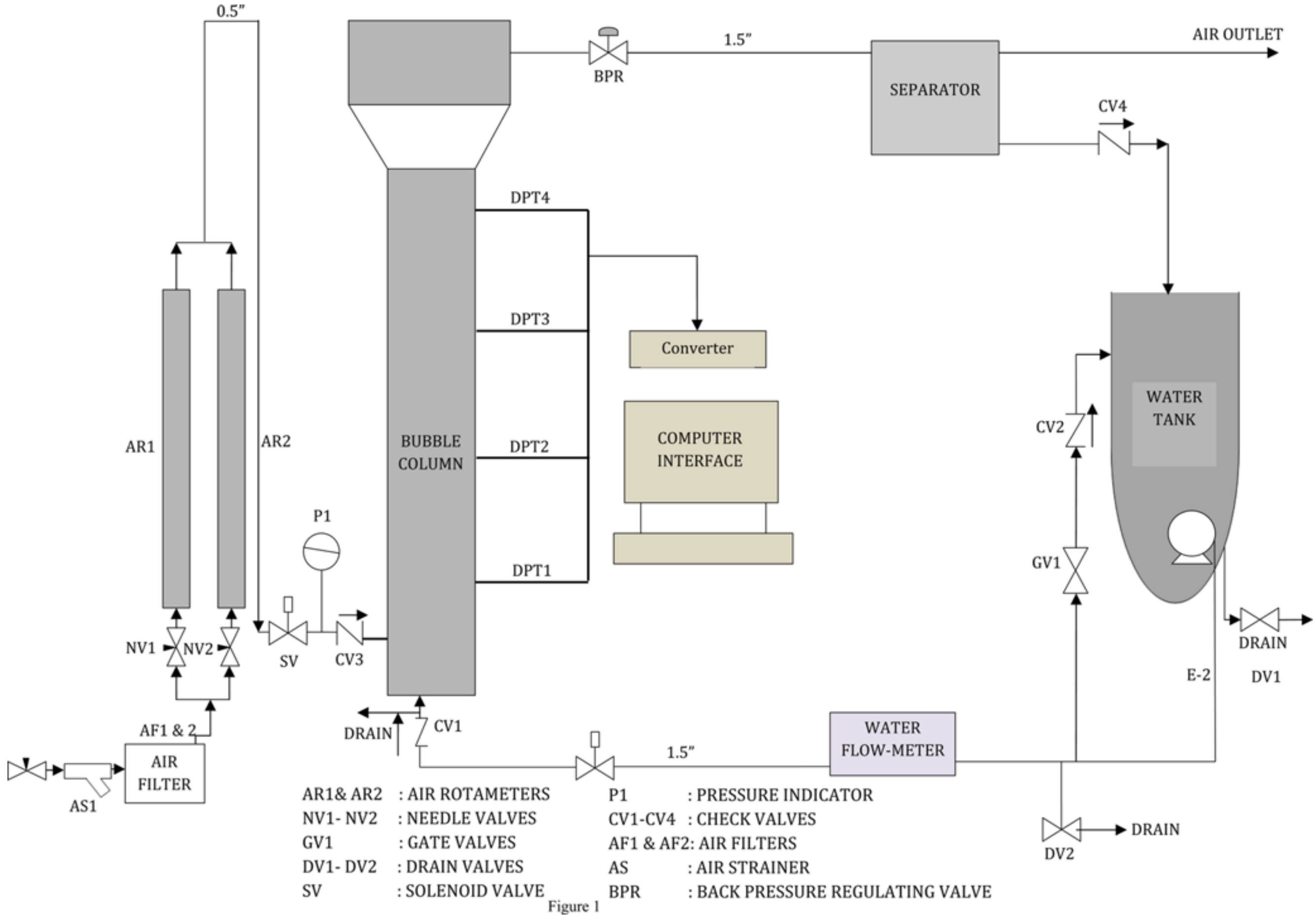


**Fig. 1. Schematic diagram of the experimental setup.**

term is the contribution due to wall shear stress, and last term is axial variation in holdup due to fluid acceleration. The contribution of the acceleration term is insignificant (~1%) for low superficial gas velocities [41]. For very high gas velocities, this term rises to ~3%. Hence, it is practical and advisable to neglect this term. Tang and Heindel approximated the wall shear stress term and derived the following equation to calculate the average gas holdup as shown in Eq. (2) [10,34].

$$\varepsilon = 1 - \frac{\Delta P}{\Delta P_{0,U_l}} \tag{2}$$

Here ΔP=is the pressure difference between the two ports of the DPT, and $\Delta P_{0,U_l}$ is the corresponding static pressure difference while gas is not flowing in the column, and keeping all other conditions unaltered. They performed various experiments to conclude that this equation has maximum 1% deviation compared to when wall stress has been modeled in Eq. (1). Eq. (2) needs just an extra experimental run, while it gives a useful approximation for the shear stress term. Hence, Eq. (2) has been used to calculate the gas holdup in the column.

Pressure fluctuations have been measured as a function of the superficial gas velocity. The distances of the DPTs are 25.3 cm, 81.3 cm, 106.6 cm and 147.3 cm from the sparger. These are piezoelectric sensors supplied by Honeywell International, USA (ST 3000 Smart Pressure Transmitter). Dynamic pressure measurements were performed at a frequency of 50 Hz for 200 seconds for each measurement. For measuring liquid/slurry flow, an electromagnetic flow meter (Model No: AQUAMAG by Krohne Marshall) was used. Air rotameter (PG-1, 2 and 8 made by Eureka Equipments) was used to measure the gas flow rate. Air line pressure was regulated by a pressure regulator. Additionally, a back pressure regulator was installed after the column to control the system pressure whenever needed.

## RESULTS AND DISCUSSION

### 1. Effect of Liquid Velocity

For three-phase co-current flows, experiments were performed with different solid concentrations up to 9% wt/vol. Fig. 2 shows that for 1% solid loading the trend is the same as in two phase flow where the holdup decreases for increasing the liquid velocity. But for higher solid loading (9%), the effect of liquid velocity over holdup is more as shown in Fig. 3. On comparing Figs. 2 and 3 one can see that the gap between the lines for superficial liquid velocity 0 and 4.08 is more in Fig. 3. It indicates that in the presence of solid the effect of liquid velocity gets enhanced. High concentration of solid particles promotes bubble coalescence, and thus decreases the holdup. In the presence of high solid loading, the slurry momentum is also more compared to two phase flows. Observation of Figs. 2 and 3 also indicates that there is a large gap between the lines for superficial liquid velocity 0 and 4.08 cm/s compared to other liquid

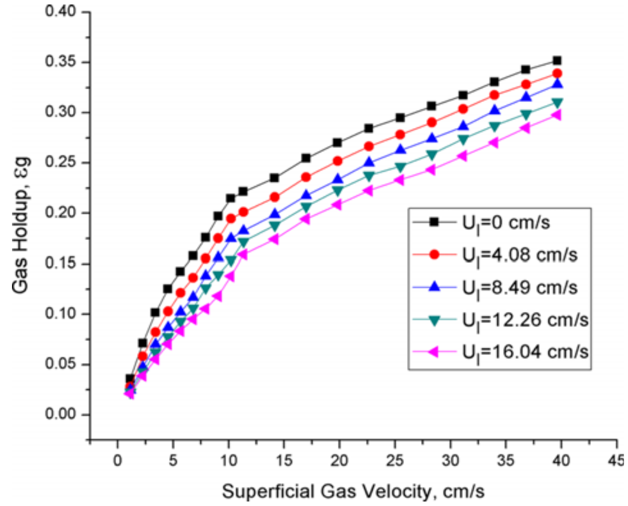


**Fig. 2. Effect of slurry velocity over gas holdup for 1% solid concentration at 1 bar.**

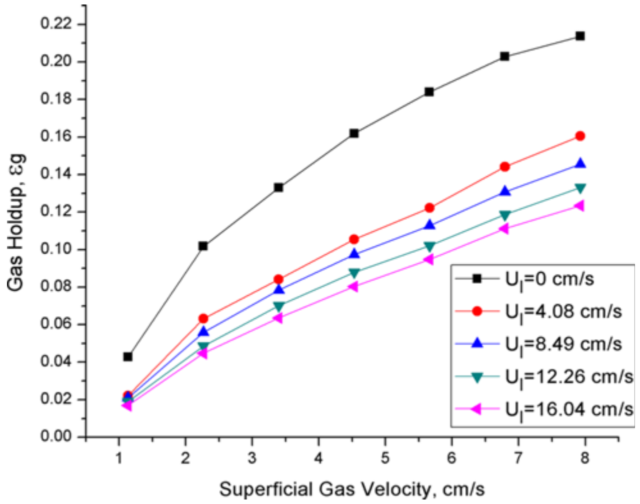


**Fig. 4. Effect of slurry velocity over gas holdup for 9% solid concentration at 5 bar.**

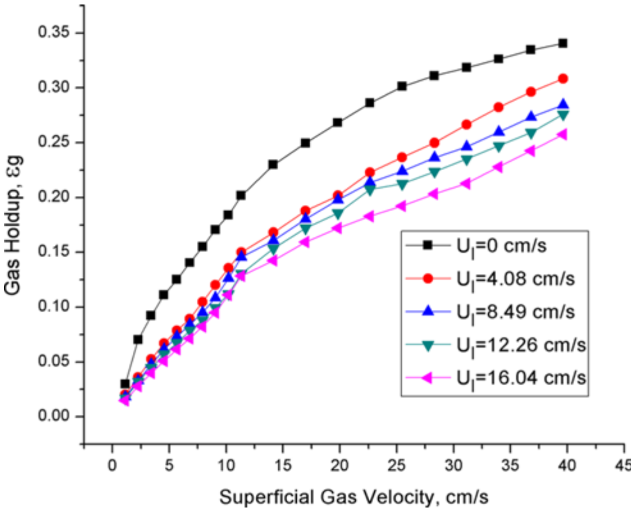


**Fig. 3. Effect of slurry velocity over gas holdup for 9% solid concentration at 1 bar.**

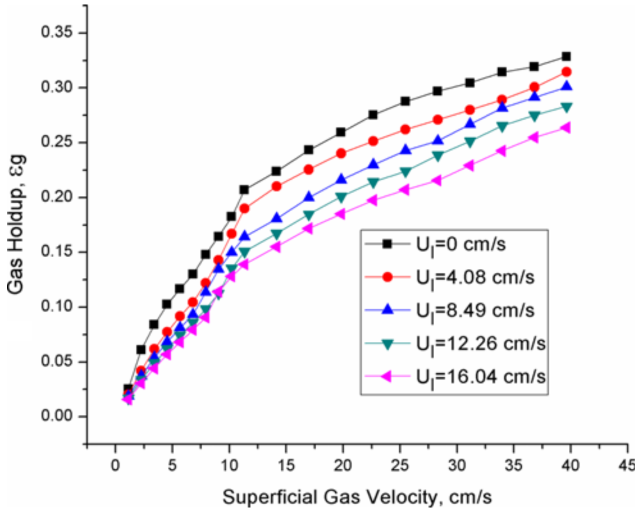


**Fig. 5. Gas holdup in homogeneous and heterogeneous regimes.**

velocities. This indicates that the hydrodynamics inside the column changes drastically as we switch from batch to co-current mode of operation. It is clear from Fig. 4 that in the co-current mode of operation, increasing the liquid velocity decreases the gas holdup at all pressures.

**2. Effect of Gas Velocity**

The gas holdup and superficial gas velocity are related by the following power-law expression [37]:

$$\varepsilon_g = k * U_g^n \quad (3)$$

As the gas velocity is increased, the gas holdup increases sharply in the homogeneous flow regime where the exponent n in Eq. (2) lies in the range of 0.7-1.2 [2]. In the heterogeneous regime, n lies in the range 0.4-0.8.

Fig. 5 is a graph for 3% solid loading showing the effect of superficial gas velocity up to 40 cm/s over gas holdup. One can clearly observe that the gas holdup increases at a faster rate initially, and the slope becomes relatively flat at a later stage. Two different slopes are visually observed in such a high range of superficial gas velocity. This change in the slope of the curve provides a rough estimate for transition from homogeneous to heterogeneous regime. Previous researchers have successfully identified various regimes in a bubble column by monitoring the evolution of a global parameter (e.g., gas holdup) or by measuring pressure fluctuations in a bubble column [40]. It has been found in the previous study that transition from homogeneous to heterogeneous regime occurs around 7 cm/s for two phase flows and delays with increasing liquid velocity [40].

**3. Drift Flux Analysis**

Zuber and Findlay [31] defined drift flux as

$$U_{drift} = (1-\varepsilon_g)U_g - (\varepsilon_g)U_l \quad (4)$$

Nacef et al. [33] proposed the following general representation of the drift flux in three-phase fluidized and fixed beds

$$U_{drift} = AU_g^b \quad (5)$$

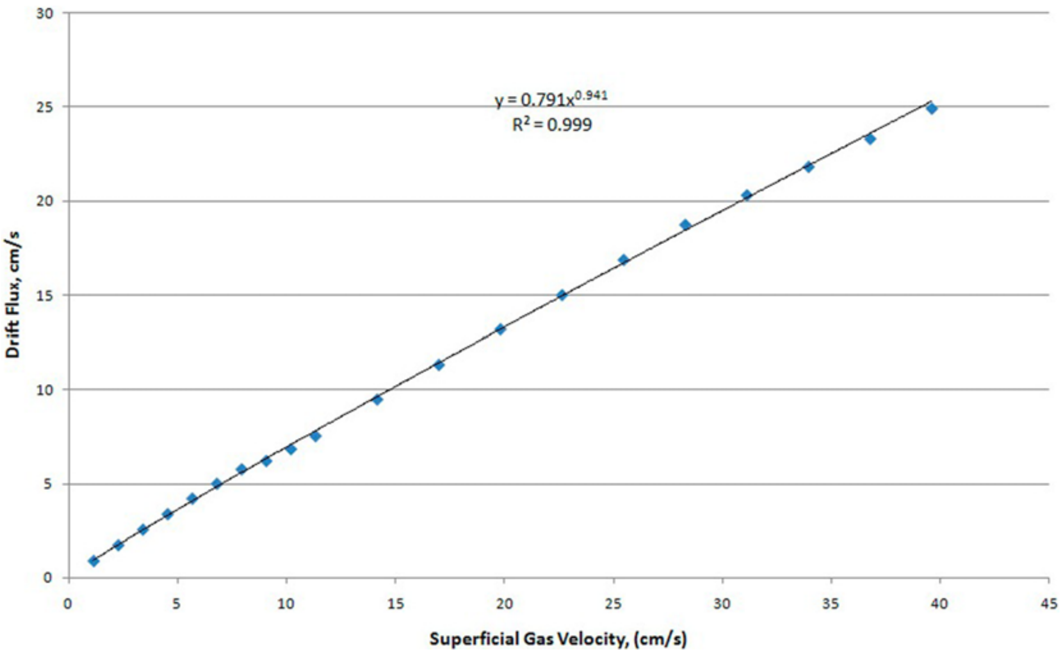


**Fig. 6. Plot of drift flux vs superficial gas velocity.**

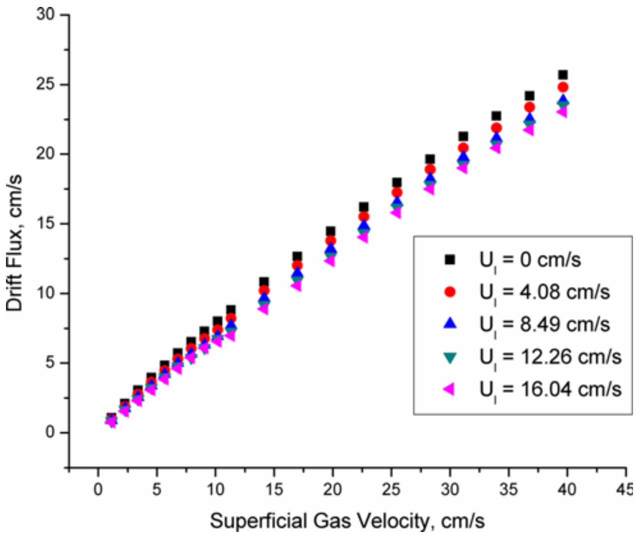


**Fig. 7. Effect of liquid velocity over drift flux for 1% solid loading.**

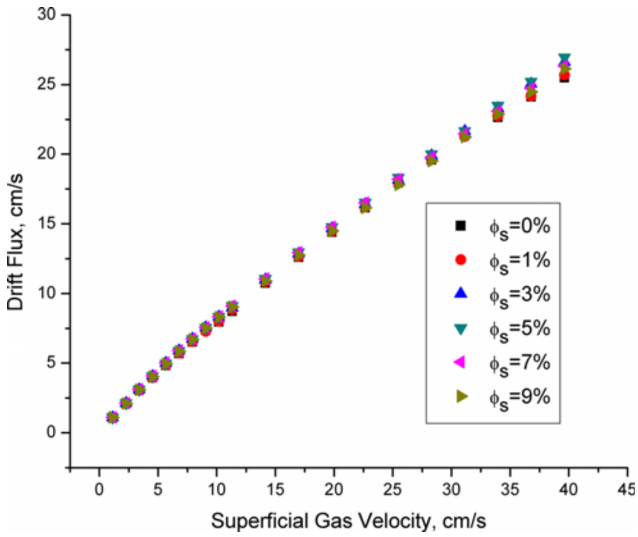


**Fig. 8. Effect of solid loading over drift flux for three phase batch column.**

The value of b is nearly unity, while A is in the range 0.5 to 0.9 [33].

A sample graph (Fig. 6) was plotted for 3% solid loading and 16.04 cm/s liquid velocity to find the value of the constant A and b. In this specific case A comes out to be 0.79, while b is 0.94. The $R^2$ for this curve is 0.999.

The effect of liquid velocity over drift flux is examined in Fig. 7 for 1% solid loading. The drift flux decreases as liquid velocity is increased. This is expected, because drift flux of a gas is its velocity relative to a surface moving with average flux. For co-current flow, increasing liquid velocity increases the velocity of the surface, thus decreasing the drift flux velocity.

To examine the effect of solid loading, drift flux was plotted for different solid concentration in batch bubble column in Fig. 8. The graph does not show any significant change in the drift flux with respect to solid loading. This is also consistent with the drift flux equation, as addition of solid has no role in determining the drift flux.

The Zuber and Findlay drift flux model is widely used for modeling gas holdup in bubble columns. It incorporates the effect of radial non-uniformity of the local flux of the mixture and the relative velocity between the two phases.

Zuber and Findlay derived that

$$\frac{\langle U_g \rangle}{\langle s_g \rangle} = C_0 \langle U_g + U_l \rangle + C_1 \quad (6)$$

where < > denotes the average over the cross section. Here, $C_0$ is called the distribution parameter and is an indicator for the radial non-uniformity of the flow. $C_1$ is the weighted mean drift flux velocity and indicates the effect of local relative velocity [10,34]. This model assumes that the radial profile for the local mixture volume flux remains constant during the fully developed flow regime, hence it ($C_0$) can be treated as constant. $C_1$ is also constant in a particular gas flow regime. This $C_1$ is equal to the terminal rise velocity of a single bubble for batch bubble column [31].

$U_g/\varepsilon_g$ vs $(U_g+U_l)$ has been plotted for two-phase batch column. By fitting a linear equation, $C_0$ is found as 2.3 in the homogeneous regime and 2.0 in the heterogeneous regime. $C_0$ is the radial distribution parameter, which is 1 for a flat profile. A value of 1.2 to 1.5 has been suggested by previous researchers in the heterogeneous regime [31,35]. In the present study, the value of $C_0$ is 2.0, which indicates that the holdup variation is large in the radial direction. Tang and Hiendel [34] also got the value of $C_0$ between 2 and 3 for his experimental study in a three-phase air-water-fiber bubble column of 15 cm diameter. In this study, $C_1$ comes out to be 0.25 m/s in the homogeneous regime and 0.31 m/s in the heterogeneous regime. Assuming the value of $C_1$ equals the terminal rise velocity of a single bubble ($V_b$), Mendelson's equation was used to calculate the average bubble radius [42].

$$V_b=\sqrt{\frac{\sigma}{\rho_l r_b}+g*r_b} \tag{7}$$

In the homogeneous regime, the average bubble radius comes out to be 4.5 mm, while in the heterogeneous regime, it is 9 mm. These two values are also consistent with the literature, as the average bubble radius in the homogeneous regime is between 1.5 to 5 mm [43]. At high superficial gas velocity the average bubble radius gets increased and it comes as 9 mm.

All the two phase data (100 data points for different liquid and gas velocities) were put under linear regression to get a correlation between the gas holdup and superficial gas and liquid velocity. The units of $U_g$ and $U_l$ are m/s in Eq. (8).

$$\frac{\langle U_g\rangle}{\langle \varepsilon_g\rangle}=2.0\langle U_g+U_l\rangle+0.223 \tag{8}$$

## 4. Effect of Pressure

The increase in pressure leads to smaller bubble sizes for three reasons: (i) the bubble size formed at sparger gets reduced [44], (ii) high pressure destabilizes the large bubbles present in the system forcing them to break into smaller bubbles [27], and (iii) the rise velocity of the bubble gets reduced in the presence of pressure [16, 24]. The residence time of a bubble increases when its velocity becomes less, leading to high gas holdup. Since pressure stabilizes the bubbly flow regime, it delays the transition to higher superficial gas velocities compared to atmospheric conditions [45,46].

Kumar et al. studied the effect of pressure for two phase flows [39]. In the present work, the effect of pressure for different superficial liquid velocities in three phase flows has been studied. This is shown in Figs. 9 and 10 for different liquid velocities and slurry concentrations.

An increase in pressure increases the holdup for a fixed slurry and gas velocity. With increase in pressure, the gas holdup initially increases and later starts getting stabilized. Thus, increasing pressure increases the gas holdup but with a tapering effect. High pressure, liquid velocity as well as solid concentration, all three play a role in determining the gas holdup. For a fixed high pressure, the trend of liquid velocity effect is similar as in the case of atmospheric pressures. The pressure increases the gas holdup irrespective of the liquid velocity and solid loading. In the presence of solid, the overall gas holdup is less compared to two phase flows. When both pressure and liquid velocity are increased, the net effect is sum total of the effect produced by these two operating parameters.

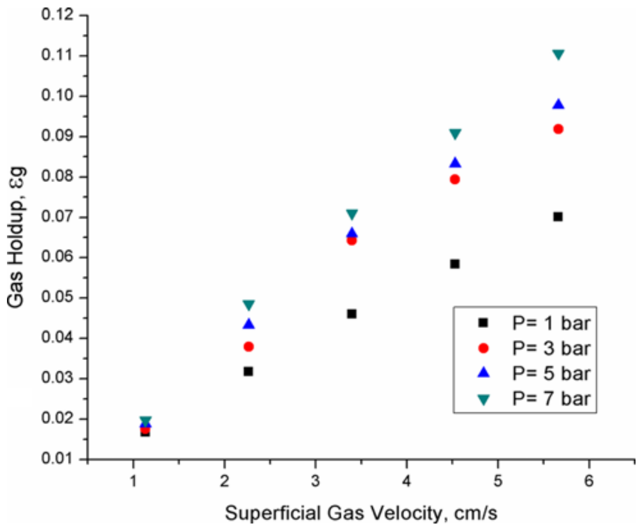


**Fig. 9. Effect of pressure over gas holdup for 5% solid loading and $U_l$=12.26 cm/s.**

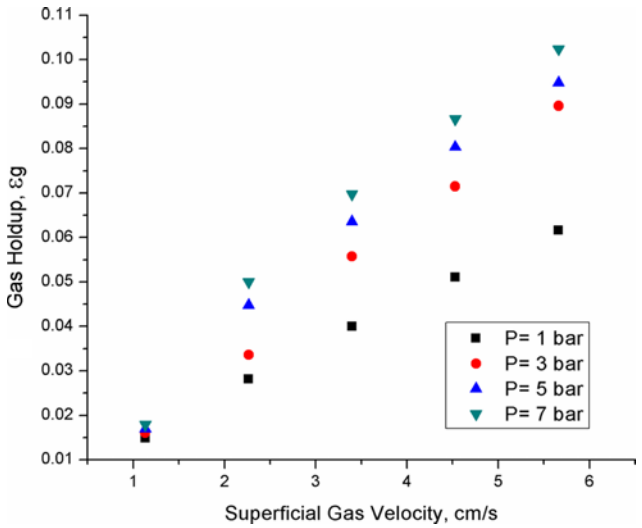


**Fig. 10. Effect of pressure over gas holdup for 9% solid loading and $U_l$=16.04 cm/s.**

To see the comparative effect of each parameter, the following model has been fitted in the data by performing regression using the MINITAB software. The coefficient of determination ($R^2$) is 0.92 for this fitting.

$$\varepsilon_g=.044*(U_g)^{0.77}*(U_l)^{-0.25}*(P)^{0.22} \tag{9}$$

In this equation superficial gas and liquid velocity are in cm/s, while operating pressure is in bar. The comparison of exponents of each term shows that superficial gas velocity affects the gas holdup most significantly. Effect of increase in pressure and liquid velocity is approximately the same in magnitude, but opposite in direction. The pressure increases the gas holdup, while increase in the liquid velocity decreases the gas holdup. For wider applicability of the correlation, Eq. (9) needs to be converted to dimensionless form. Dimensional analysis of the bubble column was done to identify the important dimensionless numbers and in terms of non-dimensional parameter, Eq. (9) takes the form as:

$$\varepsilon_g = 1.74 * 10^{-6} * \left(\frac{U_g}{U_l}\right)^{0.77} * \left(\frac{\rho_l U_l D}{\mu_l}\right)^{0.96} * \left(\frac{P}{\rho_l U_l^2}\right) \quad (10)$$

In Eq. (10), all the parameters are in SI units. Eq. (10) indicates that the ratio of superficial gas to liquid velocity, Reynolds number and Euler number (based on operating pressure) are important parameters determining the gas holdup.

## 5. Effect of Solid Concentration

Addition of solid affects the density and viscosity of the liquid. As discussed in detail by Mena et al., each particle present in the system poses a no-slip condition for the liquid, where the liquid and solid velocity must be equal [19]. It adds an extra velocity gradient and the viscous dissipation increases. This apparently increases the viscosity. In the presence of solid, various correlations have been determined to get the viscosity of solid and liquid mixture. One such model is Riquart's model [47] which determines the slurry viscosity as

$$\mu_{slurry} = \mu_l\left(1 + \varphi_s \frac{\rho_s - \rho_l}{\rho_s}\right)(1 - \varphi_s)^{-2.59} \quad (11)$$

Increasing viscosity also promotes bubble coalescence, leading to fast rising large size bubbles. This reduces the overall gas holdup.

In the present work, fine glass particles (35 mm average size) were used as solid phase in the high pressure co-current air-water system. The liquid velocity varied from 0 to 16.04 cm/s. The pressure varied from 1 bar to 7 bar. For every liquid velocity at atmospheric pressure, the gas holdup decreased much less as we moved from two phase to 1% solid loading, but afterwards a considerable decrease in holdup was observed for 3% and 5% solid loading. Beyond 5% solid loading the gas holdup still decreased, but at a much slower rate. In case of high pressure, even 1% addition of solid shows a significant change in the gas holdup. The gas holdup further decreased when solid loading was increased to 3%. No much change is observed for further increase in the solid loading. Figs. 11 and 12 show this effect of solid loading in a co-current bubble column at different pressures. Compared to Mena et al. [19], we could not get any maxima in the holdup values at high pressures or co-current atmospheric experiments. The difference in particle size and its nature should be the reason for the difference in the results. Their particle size was 2.1 mm and neutrally buoyant, while in the present case it is 35 μm fine glass beads powder with high density (2,500 kg/m$^3$). The results of atmospheric cases go hand in hand with the experiments done by Gandhi et al. [22], but they did experiments in the discrete step of 10% solid loading. They have not investigated the column in the range 1% to 10% solid loading. Also, they performed atmospheric three phase batch experiments only, while in this case

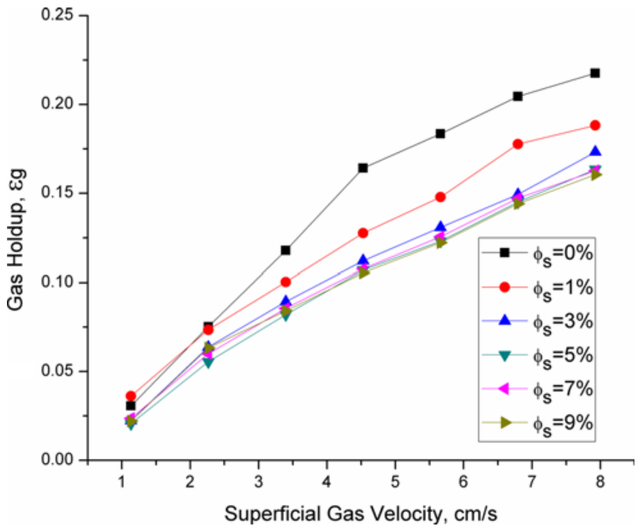


**Fig. 12. Effect of solid loading over gas holdup for $U_l$=12.26 cm/s and P=5 bar.**

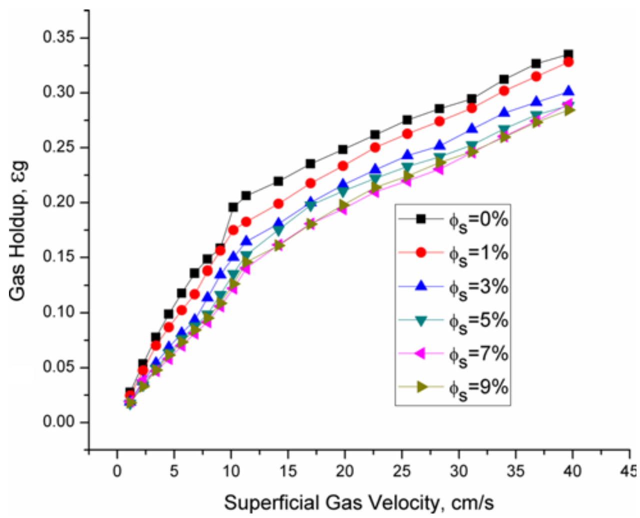


**Fig. 11. Effect of solid loading over gas holdup for $U_l$=8.49 cm/s and P=1 bar.**

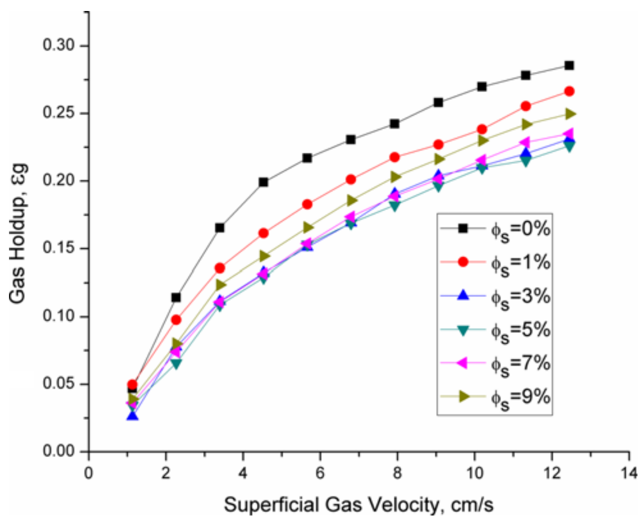


**Fig. 13. Effect of solid loading over gas holdup for $U_l$=0 cm/s and P=3 bar.**

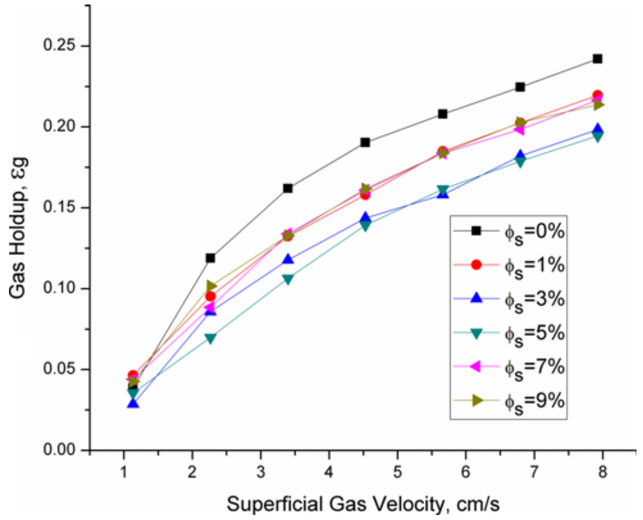


**Fig. 14. Effect of solid loading over gas holdup for $U_l$=0 cm/s and P=5 bar.**

batch and co-current experiments at various pressures have been performed.

In co-current flow, settling is not observed. But for batch three phase flow, when solid loading is 5% or more, settling starts. So, even if the loading is high, the apparent loading in the column decreases significantly. This in turn increases the holdup. For example, in Figs. 13 and 14, the gas holdup first decreases till 3% solid loading because of the solid effect discussed above. As, we move from 3% to 5% loading, settling starts playing a role, leading to apparent decrease of solid loading in the column and a corresponding increase in the gas holdup. As solid loading is further increased to 7%, solid powder starts agglomerating leading to further decrease of solid in the column. There is a negligible decrease in the gas holdup as we increase the loading from 7% to 9%.

To examine the comparative effect of each parameter in three phase flows, regression was performed again using the MINITAB software for approximately 800 data points and we got the following correlation:

$$\varepsilon_g = .032 * (U_g)^{0.82} * (U_l)^{-0.20} * (P)^{0.24} * (\varepsilon_s)^{-0.11} \quad (12)$$

In this equation superficial gas and liquid velocity are in cm/s, while operating pressure is in bar. The coefficient of determination ($R^2$) is 0.97 for this fitting. This again concludes that superficial gas velocity is the most important parameter determining the gas holdup. Solid loading is the least significant parameter that affects the gas holdup. Pressure and liquid velocity have almost same impact over gas holdup, but in the opposite direction.

Again, in terms of dimensionless parameters, Eq. (12) takes the form as:

$$\varepsilon_g = 3.60 * 10^{-7} * \left(\frac{\rho_l U_l D}{\mu_l}\right)^{1.09} * \left(\frac{U_g}{U_l}\right)^{0.820} * \left(\frac{P}{\rho_l U_l^2}\right)^{0.235} * (\varphi_s)^{-0.108} \quad (13)$$

Eq. (13) may be used to estimate gas holdup for intermediate values of superficial gas and liquid velocities, pressures and solid loadings. Equations in dimensionless form are very helpful for design and scale up of a bubble column.

## SUMMARY AND CONCLUSIONS

The effect of gas and liquid velocity, solid concentration, and operating pressure has been studied experimentally in a 15 cm diameter air-water-glass beads bubble column. The pressure was varied from 1 to 7 bar. For low superficial gas velocity the effect of slurry velocity on gas holdup was less. For higher superficial gas velocities, gas holdup decreased with increase in the slurry velocity. The hydrodynamics inside the column changed drastically as we switched from batch to co-current mode of operation leading to a sharp decrease in the gas holdup. In the co-current mode of operation for three phase flows, increasing the slurry velocity decreased the gas holdup at all pressures. By increasing the superficial gas velocity, the gas holdup first increased sharply and then slope became relatively flat at a later stage. These two different slopes are visually observed in graphs containing large range of superficial gas velocities. For co-current three phase flows, the gas holdup decreased as we moved from two phase to 1%, 3% and 5% solid loading. Beyond 5% solid loading the gas holdup still decreased but at a much slower rate. For batch three phase flow, when solid loading was 5% or more, settling started. Thus, even if the loading is high, the actual loading in the column decreases significantly. This leads to higher gas holdup for high solid loading in case of 7% and 9% solid loading. Increase in the pressure increased the gas holdup for all the cases. Moving from atmospheric conditions to higher pressure, the gas holdup increased very fast initially and later on this increment was small. Thus, increasing superficial gas velocity and pressure increases the gas holdup, while increasing liquid velocity and solid concentration decreases the holdup. Drift flux analysis of the bubble column was performed and a correlation was developed for gas holdup as a function of superficial gas and liquid velocities. The bubble diameter and its terminal rise velocity were also estimated for both homogeneous and heterogeneous regime. Drift flux decreased with increase in slurry velocity. For batch three phase systems, addition of solids had no effect over drift flux. For both two and three phase flows, correlations were developed by regression analysis to estimate gas holdup as a function of various operating parameters. For wider applicability of the correlation, it was converted into non-dimensional form. Comparison of exponents of various terms in the correlation indicates that the superficial gas velocity is the most significant parameter that determines the gas holdup. Solid loading is the least significant parameter affecting the gas holdup. Pressure and liquid velocity have almost same impact, but in the opposite direction. When more than one parameter is present in the system, the net effect is a sum total of the effect produced by all the parameters.

## LIST OF SYMBOLS

Dc : diameter of the column
g : acceleration due to gravity
P : operating pressure
$r_b$ : bubble radius
$U_g$ : superficial gas velocity
$U_l$ : superficial liquid velocity
$U_{drift}$ : drift velocity

$U_{slip}$ : slip velocity
$V_b$ : terminal rise velocity
$\varepsilon_g$ : gas holdup
$\varphi_s$ : solid loading
$\mu_l$ : liquid viscosity
$\sigma$ : surface tension
$\rho_l$ : liquid density
$\rho_s$ : solid density
$\tau_w$ : wall shear stress

## ACKNOWLEDGEMENTS

The authors acknowledge the financial support provided by Chevron, USA; Advanced Refining Technologies (ART), USA and Hindustan Petroleum Corporation Limited (HPCL), India.

## REFERENCES

1. S Degaleesan, M Dudukovic and Y Pan, *AIChE J.*, **47**, 1913 (2001).
2. Y. T. Shah, S. P. Godbole and W. D. Deckwer, *AIChE J.*, **28**, 353 (1982).
3. H. Li and A. Prakash, *Ind. Eng. Chem. Res.*, **36**, 4688 (1997).
4. W. D. Deckwer and A. Schumpe, *Chem. Eng. Sci.*, **48**, 889 (1993).
5. Y. T. Shah, A. A. Kulkarni, J. H. Wieland and N. L. Carr, *Chem. Eng. J.*, **26**, 95 (1983).
6. J. Zahradnik, M. Fialova, M. Ruzicka, J. Drahos, F. Kastanek and N. H. Thomas, *Chem. Eng. Sci.*, **52**, 3811 (1997).
7. T. J. Lin, K. Tsuchiya and L. S. Fan, *AIChE J.*, **44**, 545 (1998).
8. P. D. Hol and T. J. Heindel, *Ind. Eng. Chem. Res.*, **44**, 4778 (2005).
9. H. M. Letzel, J. C. Schouten, R. Krishna and C. M. van den Bleek, *Chem. Eng. Sci.*, **54**, 2237 (1999).
10. C. Tang and T. J. Heindel, *Chem. Eng. Sci.*, **61**, 3299 (2006).
11. C. Tang and T. J. Heindel, *Chem. Eng. Sci.*, **59**, 623 (2004).
12. S. Kara, B. G. Kelkar, Y. T. Shah and N. L. Carr, *Ind. Eng. Chem. Pro. Des. Dev.*, **21**, 584 (1982).
13. A. S. Khare and J. B. Joshi. *Chem. Eng. J.*, **44**, 11 (1990).
14. B. G. Kelkar, Y. T. Shah and N. L. Carr, *Ind. and Eng. Chem. Pro. Des. and Dev.*, **23**, 308 (1984).
15. J. W. A. De Swart, R. E. Van Vliet and R. Krishna, *Chem. Eng. Sci.*, **51**, 4619 (1996).
16. L. S. Fan, G. Q. Yang, D. J. Lee, K. Tsuchiya and X. Luo, *Chem. Eng. Sci.*, **54**, 4681 (1999).
17. R. Krishna, J. Ellenberger and C. Maretto, *Int. Commun. Heat Mass Trans.*, **26**, 467 (1999).
18. S. Banisi, J. A. Finch, A. R. Laplante and M. E. Weber, *Chem. Eng. Sci.*, **50**, 2329 (1995).
19. P. C. Mena, M. C. Ruzicka, F. A. Rocha, J. A. Teixeira and J. Drahos, *Chem. Eng. Sci.*, **60**, 6013 (2005).
20. K. Tsuchiya, A. Furumoto, L. S. Fan and J. Zhang, *Chem. Eng. Sci.*, **52**, 3053 (1997).
21. X. Luo, J. Zhang, K. Tsuchiya and L. S. Fan, *Chem. Eng. Sci.*, **52**, 3693 (1997).
22. B. Gandhi, A. Prakash and M. A. Bergougnou, *Powder Technol.*, **103**, 80 (1999).
23. X. Su and T. J. Heindel, *Can. J. Chem. Eng.*, **81**, 412 (2003).
24. R. Krishna, J. W. A. De Stewart, J. Ellenberger, G. B. Martina and C. Maretto, *AIChE J.*, **43**, 311 (1997).
25. S. Kumar, P. Munshi and A. Khanna, *Procedia Engineering*, **42**, 782 (2012).
26. M. H. Oyevaar, R. Bos and K. R. Westerterp, *Chem. Eng. Sci.*, **46**, 1217 (1992).
27. H. M. Letzel, J. C. Schouten, C. M. Van den Bleek and R. Krishna, *AIChE J.*, **44**, 2333 (1998).
28. Y. Li, J. Zhang and L. S. Fan, *Chem. Eng. Sci.*, **55**, 4597 (2000).
29. A. Kemoun, B. C. Ong, P. Gupta, M. H. Al-Dahhan and M. P. Dudukovic, *Int. J. Multiphase Flows*, **27**, 929 (2001).
30. A. Behkish, R. Lemoine, L. Sehabiague, R. Oukaci and B. I. Morsi, *Chem. Eng. J.*, **127**, 69 (2007).
31. N. Zuber and J. A. Findlay, *Int. J. Heat Transfer*, **87**(C), 453 (1965).
32. G. B. Wallis *One-dimensional two-phase flow*, McGraw-Hill, NY, USA (1969).
33. S. Nacef, S. Poncin, A. Bouguettoucha and G. Wild, *Chem. Eng. Sci.*, **62**, 7530 (2007).
34. C. Tang and T. J. Heindel, *Int. J. Multiphase Flow*, **32**, 850 (2006).
35. N. N. Clark, J. W. V. Egmond and E. P. Nebiolo, *Int. J. Multiphase Flow*, **16**, 261 (1990).
36. J. R. Inga and B. I. Morsi, *Energy Fuels*, **10**, 566 (1996).
37. W. D. Deckwer, John Wiley and Sons, NY (1992).
38. J. M. Fox, *Catal. Lett.*, **7**, 281 (1990).
39. S. Kumar, P. Munshi and A. Khanna, *Procedia Engineering*, **42**, 842 (2012).
40. S. Kumar, N. Srinivasulu, P. Munshi and A. Khanna, *Can. J. Chem. Eng.*, **91**, 516 (2013).
41. J. C. Merchuk and Y. Stein, *AIChE J.*, **27**, 377 (1981).
42. H. D. Mendelson, *AIChE J.*, **13**, 250 (1967).
43. V. V. Ranade, *Computational flow modeling for chemical reactor engineering*, Academic Press, USA (2002).
44. D. H. Yoo, H. Tsuge, K. Terasaka and K. Mizutani, *Chem. Eng. Sci.*, **52**, 3701 (1997).
45. Y. Kang, Y. J. Cho, K. J. Woo, K. I. Kim and S. D. Kim, *Chem. Eng. Sci.*, **55**, 411 (2000).
46. Y. Kang, Y. J. Cho, K. J. Woo and S. D. Kim, *Chem. Eng. Sci.*, **54**, 4887 (1999).
47. G. Hillmer, L. Weismantel and H. Hofmann, *Chem. Eng. Sci.*, **49**, 837 (1994).

# Supporting Information

## Experimental analysis and development of correlations for gas holdup in high pressure slurry co-current bubble columns

**Shyam Kumar and Ashok Khanna**†

Department of Chemical Engineering, IIT Kanpur, UP-208016, India

(*Received 20 September 2013 • accepted 21 April 2014*)

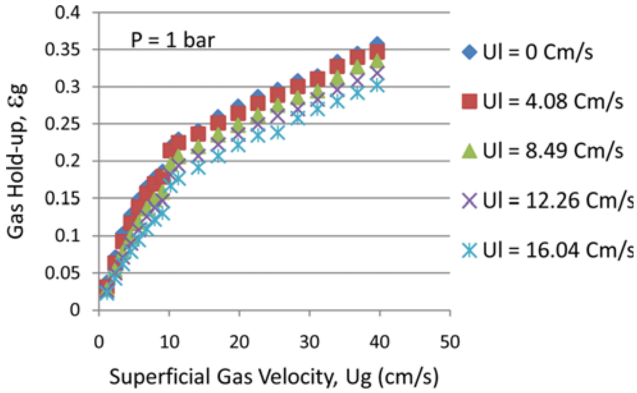


**Fig. 1. Gas holdup at 0% solid loading and 1 bar pressure.**

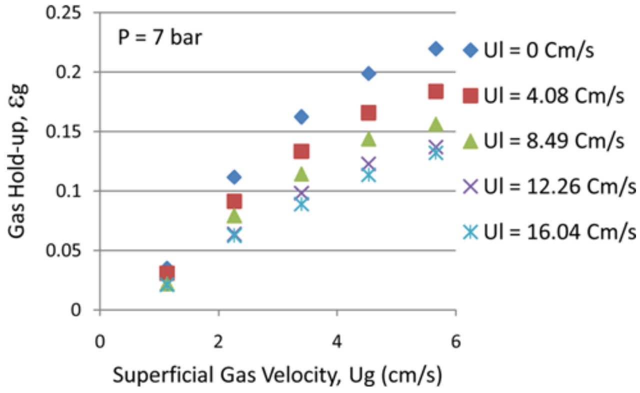


**Fig. 4. Gas holdup at 0% solid loading and 7 bar pressure.**

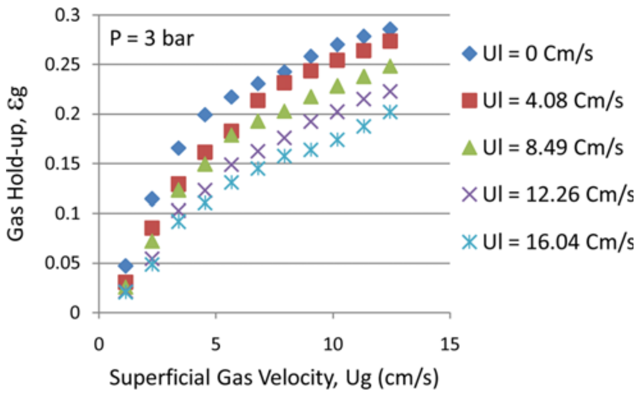


**Fig. 2. Gas holdup at 0% solid loading and 3 bar pressure.**

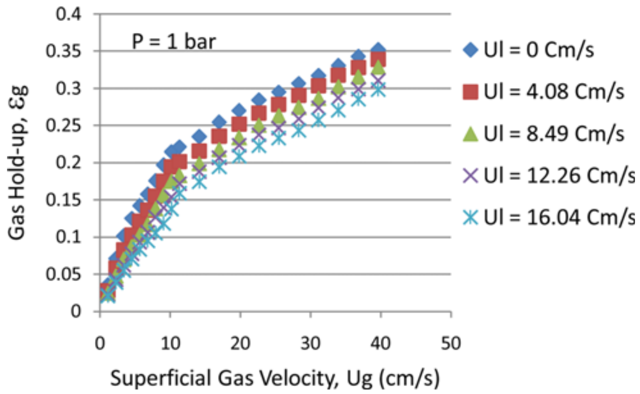


**Fig. 5. Gas holdup at 1% solid loading and 1 bar pressure.**

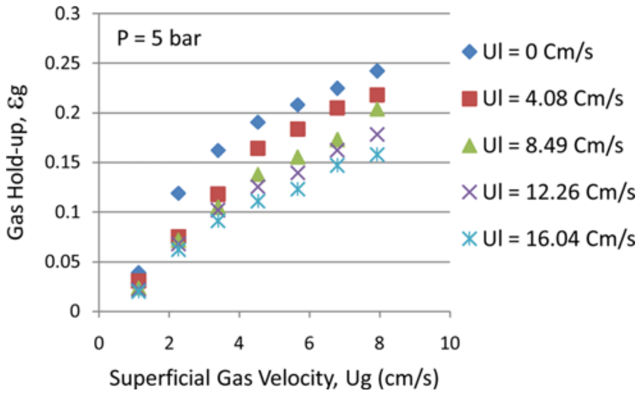


**Fig. 3. Gas holdup at 0% solid loading and 5 bar pressure.**

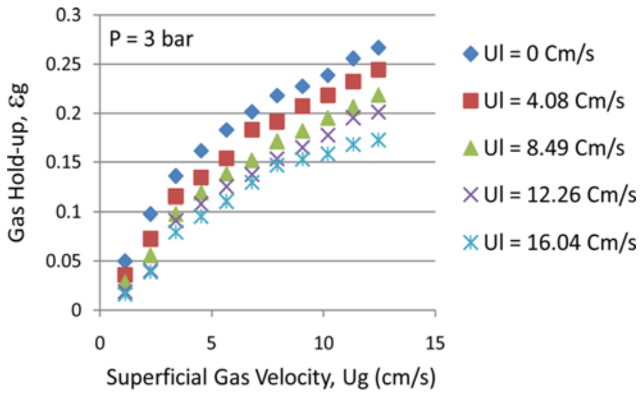


**Fig. 6. Gas holdup at 1% solid loading and 3 bar pressure.**

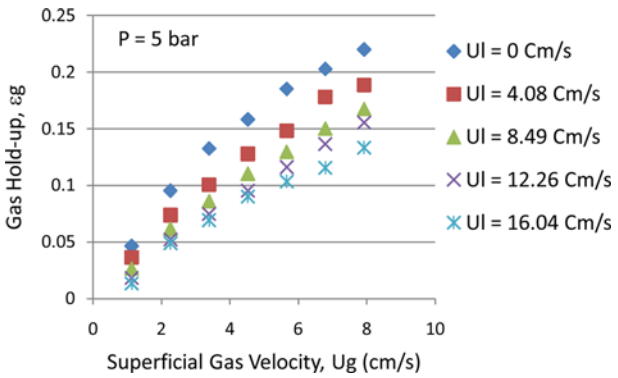


**Fig. 7. Gas holdup at 1% solid loading and 5 bar pressure.**

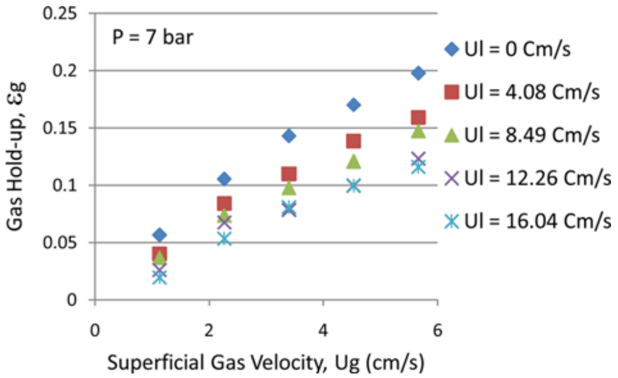


**Fig. 8. Gas holdup at 1% solid loading and 7 bar pressure.**

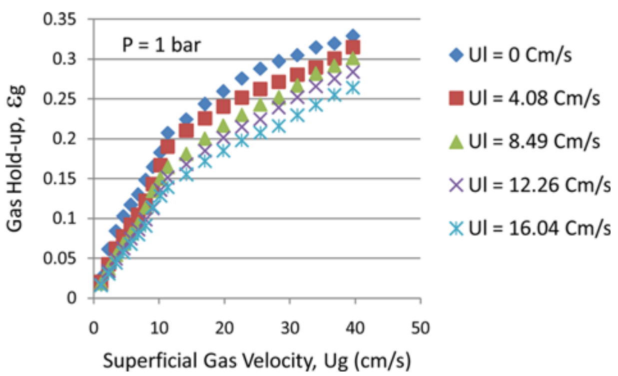


**Fig. 9. Gas holdup at 3% solid loading and 1 bar pressure.**

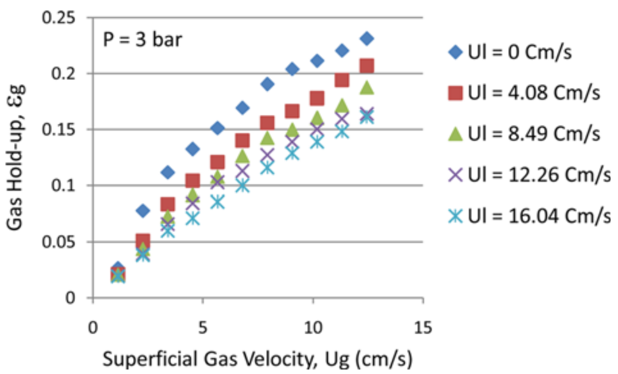


**Fig. 10. Gas holdup at 3% solid loading and 3 bar pressure.**

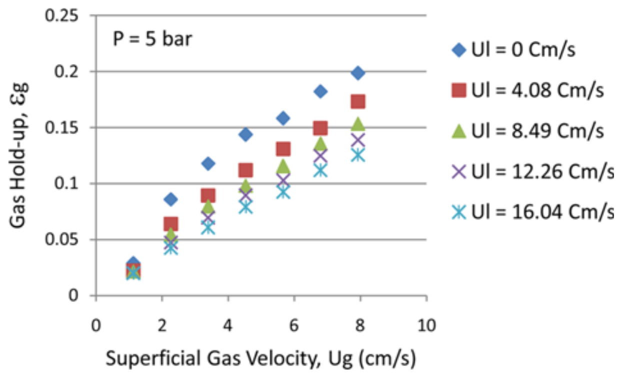


**Fig. 11. Gas holdup at 3% solid loading and 5 bar pressure.**

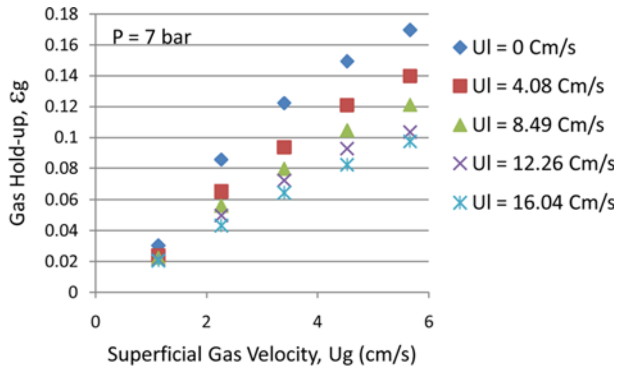


**Fig. 12. Gas holdup at 3% solid loading and 7 bar pressure.**

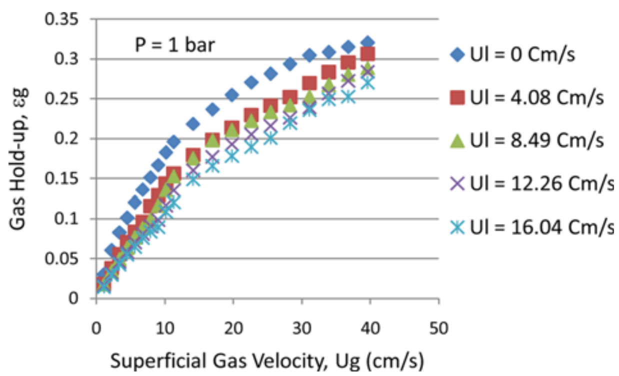


**Fig. 13. Gas holdup at 5% solid loading and 1 bar pressure.**

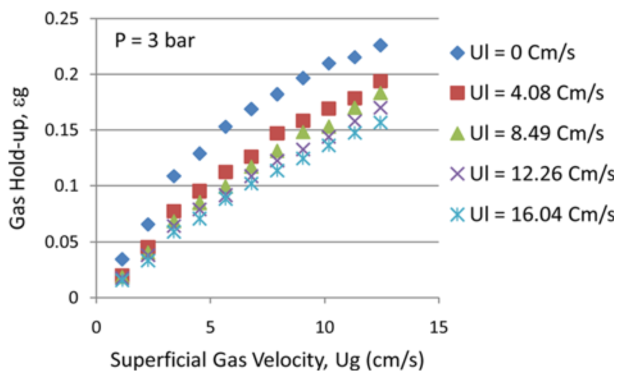


**Fig. 14. Gas holdup at 5% solid loading and 3 bar pressure.**

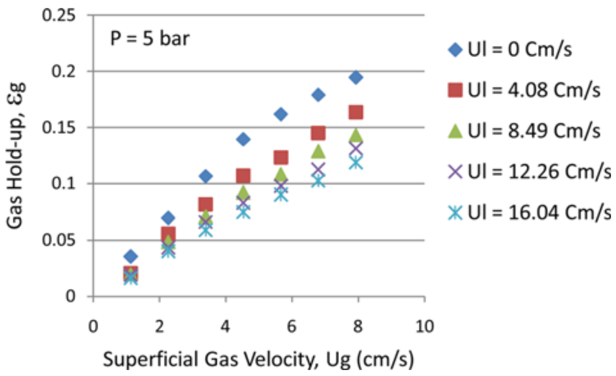


**Fig. 15. Gas holdup at 5% solid loading and 5 bar pressure.**

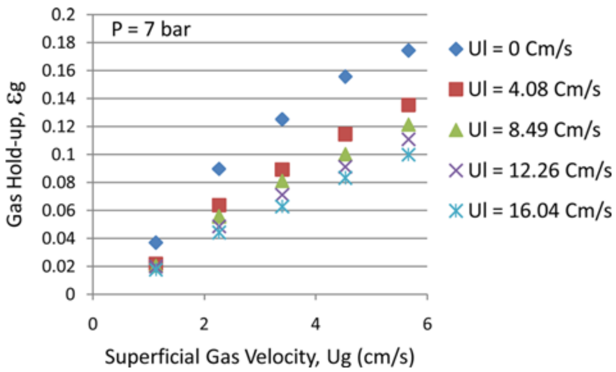


**Fig. 16. Gas holdup at 5% solid loading and 7 bar pressure.**

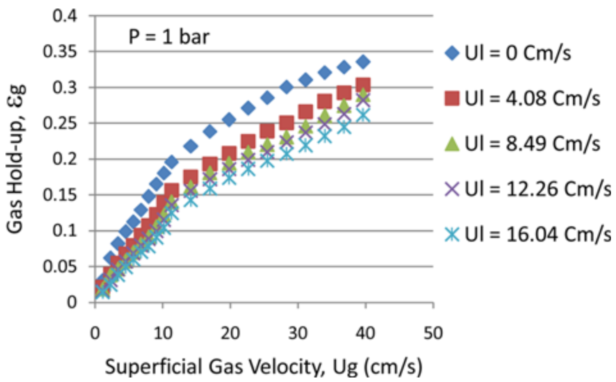


**Fig. 17. Gas holdup at 7% solid loading and 1 bar pressure.**

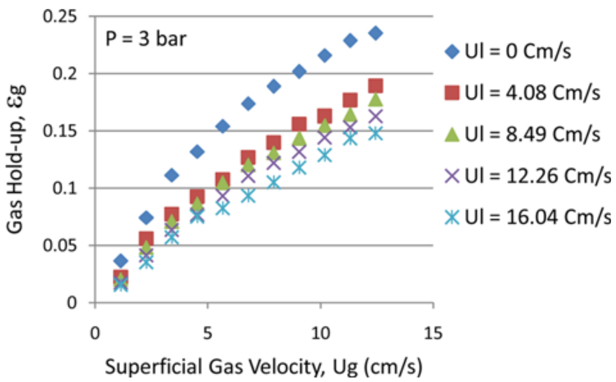


**Fig. 18. Gas holdup at 7% solid loading and 3 bar pressure.**

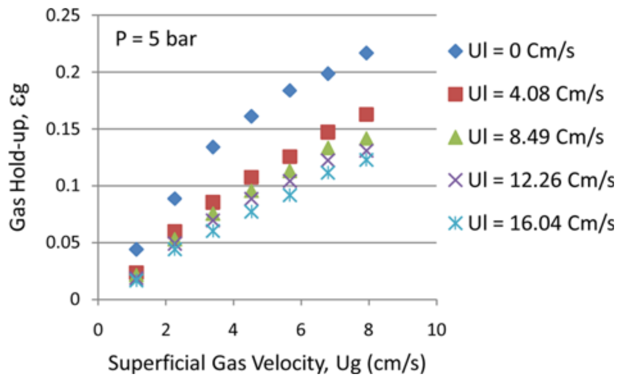


**Fig. 19. Gas holdup at 7% solid loading and 5 bar pressure.**

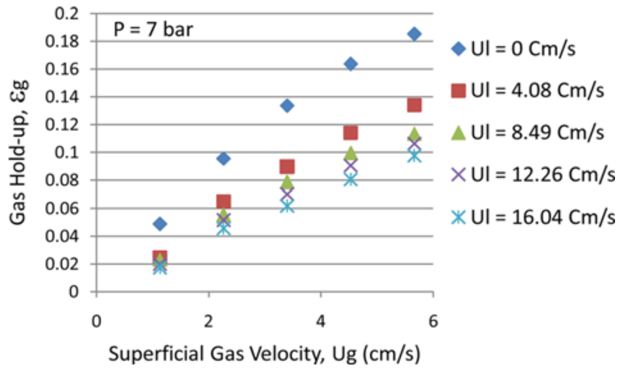


**Fig. 20. Gas holdup at 7% solid loading and 7 bar pressure.**

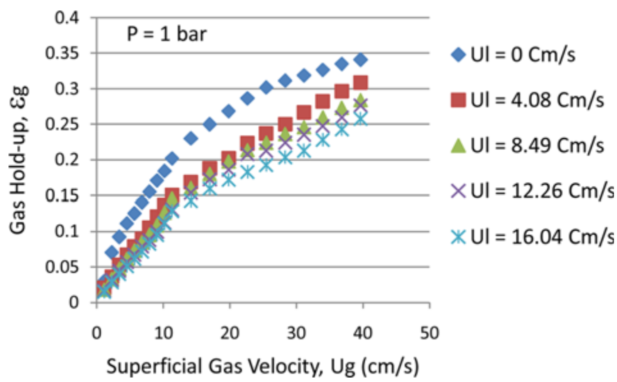


**Fig. 21. Gas holdup at 9% solid loading and 1 bar pressure.**

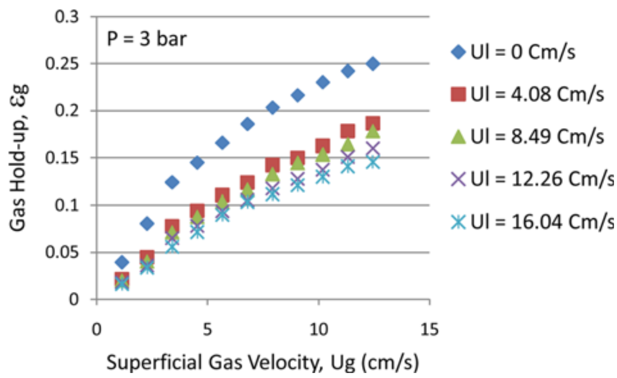


**Fig. 22. Gas holdup at 9% solid loading and 3 bar pressure.**

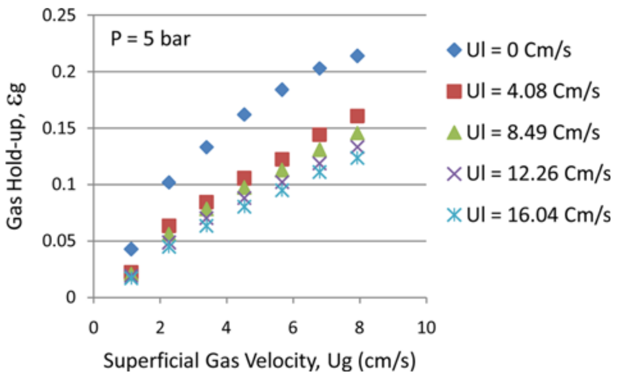


**Fig. 23. Gas holdup at 9% solid loading and 5 bar pressure.**

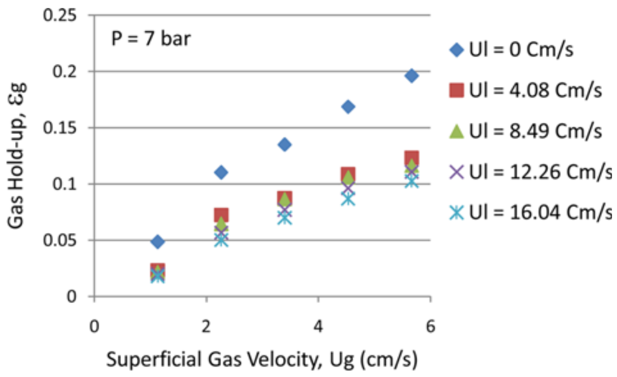


**Fig. 24. Gas holdup at 9% solid loading and 7 bar pressure.**